A GPS-Based Decentralized Control Method for Islanded Microgrids

Golsorkhi, Mohammad; Lu, Dylan; Guerrero, Josep M.

Published in:
I E E E Transactions on Power Electronics

DOI (link to publication from Publisher):
10.1109/TPEL.2016.2551265

Publication date:
2017

Document Version
Early version, also known as pre-print

A GPS-Based Decentralized Control Method for Islanded Microgrids

Mohammad S. Golsorkhi, *Graduate Student Member, IEEE,* Dylan D.C. Lu, *Senior Member, IEEE, and* Josep M. Guerrero, *Fellow, IEEE*

Abstract— Coordinated control of distributed energy resources (DER) is essential for the operation of islanded microgrids (MGs). Conventionally, such coordination is achieved by drooping the frequency of the reference voltage versus active (or reactive) power. The conventional droop method ensures synchronized operation and even power sharing without any communication link. However, that method produces unwanted frequency fluctuations, which degrade the power quality. In order to improve the power quality of islanded MGs, a novel decentralized control method is proposed in this paper. In this method, GPS timing technology is utilized to synchronize the DERs to a common reference frame, rotating at nominal frequency. In addition, an adaptive Q-f droop controller is introduced as a backup to ensure stable operation during GPS signal interruptions. In the context of the common reference frame, even sharing of active (i_d) and reactive (i_q) components of current are achieved based on v_d-i_d and v_q-i_q droop characteristics. The method has been tested on laboratory scale MG. Experimental results demonstrate the efficacy of the proposed method in terms of dynamics, power quality and robustness with respect to GPS interruptions.

***Index Terms*— Control, Dispersed storage and generation, Global Positioning System, Power quality, Robustness.**

I. Introduction

STABLE and reliable operation of islanded microgrids (MGs) requires a coordinated control of individual distributed energy resources (DERs) [1]. Conventionally, such coordination is achieved by means of the droop control method. In this method, the frequency and amplitude of the DER reference voltage are drooped according to the average active and reactive power, respectively. By selecting appropriate droop coefficients, the load power is shared between the DERs according to the corresponding ratings [2].

An intrinsic feature of the conventional droop method is the dependency of the frequency on the loading conditions [3]. This results in unwanted frequency deviations which degrade the power quality. The frequency deviations can be compensated by two different approaches:

1-Secondary control schemes: In this approach, which is inspired by secondary control method in power systems, a central controller sends a frequency compensation signal to the DERs. The signal is used by the local controllers to shift the local P-f droop characteristics[4]. So, the steady-state frequency is restored to the nominal value [5]. However, the implementation of the secondary control level requires communication links among the DERs. In addition, the method does not prevent transient frequency fluctuations subsequent to load changes. In case of power systems, such transients are negligible due to the smoothness of load changes. However, in islanded MGs the relatively larger magnitude of instantaneous load changes results in considerable frequency fluctuations.

2- Control methods based on GPS synchronization: An alternative approach is using GPS timing technology [6] to realize constant frequency operation. In this approach, each DER is equipped with a GPS receiver, which produces a pulse at frequency of 1Hz (1PPS). Since all GPS receivers are locked to atomic clocks of the GPS satellites, the 1PPS signal can be utilized to synchronize the DERs.

Recently, several MG control methods based on GPS have been proposed. In [7], a power-angle (P-δ) droop characteristic is introduced to coordinate the power generation of the DERs according to the voltage angles. However, this method suffers from slow dynamic response due to the intrinsic delay of power measurement. In [8], a power management system (PMS) is proposed to calculate the amplitude and angle of the reference voltages of individual DERs according to the power flow requirements. The reference values are then communicated to the local controllers, which regulate the inverter voltages. However, this method requires communication links among DERs. In [9], a decentralized plug and play (P'n'P) control method is proposed to ensure stable operation of meshed MGs subsequent to connection/disconnection of new DERs. However, the requirements of line parameters and load current feedback make the method difficult to implement. In [10], the GPS timing is used to synchronize the rotating reference frames (SRRFs) of the local controllers. The DERs are then coordinated by drooping the d and q axis components of the reference voltage with respect to the d and q axis components of current, respectively.

So far, the GPS-based MG control methods have been studied using computer simulations [7]-[10]. Therefore, the practical issues concerning GPS synchronization have been largely neglected. The most important issue is the interruption of the GPS signal, which might result in circulating currents between the DERs or instability depending on the duration of interruption. Another issue is the interfacing of the GPS receivers with the local controllers.

In this paper, a novel decentralized control method has been proposed to enable practical implementation of GPS timing technology in MG control applications. In this method, the DERs are synchronized by using a combination of GPS timing and an adaptive Q-f droop characteristics. Under normal operating conditions, the DERs are synchronized based on the

M.S. Golsorkhi and Dylan D. C. Lu are with the School of Electrical and Information Engineering, University of Sydney, NSW2006, Australia.(e-mail: mohammad.golsorkhiesfahani@sydney.edu.au; dylan.lu@sydney.edu.au). J. M. Guerrero is with the Department of Energy Technology, Aalborg University, 9220 Aalborg East, Denmark (Tel: +45 2037 8262; Fax: +45 9815 1411; e-mail: joz@et.aau.dk).

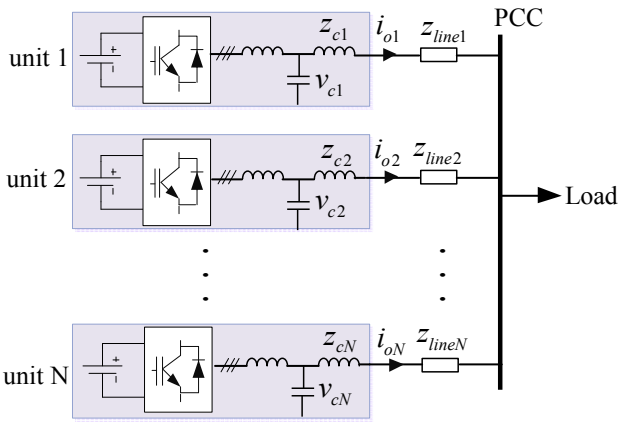

Fig. 1. Schematic diagram of an islanded ac MG.

GPS signals and the frequency is fixed at the nominal value. In case that the GPS signal of a DER fails, the backup Q-f droop is activated to maintain synchronization with other DERs. The synchronization scheme does not require any information about the availability of GPS signal at other DER units. In addition, stable operation is guaranteed regardless of the number of DERs with GPS failure. The scheme is used along with V-I droop control method, to enable coordinated operation without any communication link among DERs.

The salient features of the proposed control strategy in comparison with the previous schemes are summarized in Table I. In this table "Y" and "N" denote yes and no, respectively. Similar to P-δ [7] and V-I [10] droop schemes, the proposed method is independent from network topology/impedances and does not require a communication link between the units. Unlike the other methods, the proposed strategy is robust with respect to GPS failure. In terms of frequency regulation, fixed frequency operation is achieved as long as GPS receivers are functional. However, in case that several units experience GPS failure, the frequency is changed to guarantee safe operation.

The rest of the paper is organized as follows: The motivation of utilizing GPS technology for MG control applications is addressed in Section II. In Section III, the fundamental of GPS time synchronization is explained. The proposed method is detailed in Section IV. The small signal stability of the method is studied in Section V. Experimental results are presented in Section VI to verify the efficacy of the method. Section VII concludes the paper.

II. Synchronization of Parallel Inverters in MGs

Consider the islanded ac MG of Fig. 1. The MG is supplied by of N voltage-source DER units, which are connected to the point of common coupling (PCC) through line impedances. Each DER is comprised of a DC energy source, a power electronic inverter and a passive filter. The inverter voltage is controlled by means of a cascaded voltage-current control loop, which regulates the filter capacitor voltage, v_c, to its reference value [11]. The output current of DER unit k (k = 1,2,…,N) is calculated as

$$i_k = \frac{v_{ck} - v_{PCC}}{z_{ck} + z_{linek}} \tag{1}$$

in which v_{PCC}, z_{ck} and z_{linek} are the PCC voltage, output inductor impedance and line impedance of unit k, respectively.

TABLE I
Comparison of the Proposed Method with the Existing Schemes

Feature \ Method	PMS [8]	P'n'P [9]	P-δ [7]	V-I [10]	Proposed
Works without any communication among DERs	N	Y	Y	Y	Y
Independent from network topology/ impedances	N	N	Y	Y	Y
Has a fast dynamic response	Y	Y	N	Y	Y
Experimental results provided	N	N	N	N	Y
Robust to GPS failure	N	N	N	N	Y
Frequency of operation	Fixed	Fixed	Fixed	Fixed	Fixed/Var.

Equation (1) implies that the current of each unit is dependent on the corresponding capacitor voltage. Stable operation of the MG requires the reference voltages of the units to be in synchronism with each other. Conventionally, such synchronization is achieved by using droop control method. In this method, the reference frequency of each DER is obtained from an active power- frequency (P-f) droop characteristic, as follows:

$$f = f_0 - nP \tag{2}$$

where f, f_0, n are the reference and nominal frequency and droop coefficient, respectively. Moreover, P is the average active power, which is calculated as

$$P = \frac{\omega_{cp}}{s + \omega_{cp}} p \tag{3}$$

in which ω_{cp} and p are the instantaneous power and cut-off frequency of the low pass filter, respectively. The low pass filter in (3) introduces a virtual inertia in the system and the P-f droop characteristic acts like a negative feedback, which stabilizes the system [12]. At the same time, it enables proportional sharing of the load between the DERs. However, the dependency of the frequency on load makes this method inferior in terms of power quality.

An alternative approach is fixing the frequency of the reference voltages at the rated value and coordinating the reference angles so as to achieve proper load sharing. This strategy necessitates the use of a common time reference by each of the DER units. Given the distributed nature of the MGs and the required timing accuracy, GPS timing technology has been proposed as the practical solution [7]-[10]. The fundamentals of GPS timing and its application for angle synchronization of DERs are detailed in the Section III.

III. GPS Time Synchronization

A. Fundamentals

Although GPS is mainly known as a navigation system, it is also an accurate timing system. In fact, GPS uses timing signals to obtain the position. GPS receivers obtain the position based on the following equation [13]:

$$\sqrt{(x_i - u_x)^2 + (y_i - u_y)^2 + (z_i - u_z)^2} = c(\Delta t_i - t_b) \tag{4}$$

where, (x_i , y_i , z_i) are the coordinates of satellite i , (u_x , u_y , u_z) are the coordinates of the receiver, Δt_i is the time shift of the signal received from satellite i, t_b is the bias of the receiver clock with respect to the Universal Coordinated Time (UTC), and c is the speed of light. The unknown variables in (4) are the coordinates of the receiver as well as the bias of the receiver clock. Expressing (4) for four different satellites, a system of four non-linear equations with four unknown variables is obtained. The equations are then solved by using an iterative method to obtain the receiver location as well as the receiver clock bias. The time bias can be used to accurately compute the UTC time.

For the application of time synchronization in MGs, the receiver position is fixed after installation. Therefore, the receiver position can be calculated once and stored in the memory. Afterwards, only the clock bias of the receiver needs to be computed. So, only one of the eight observable satellites is sufficient for the application. It should be pointed out the clock bias is a dynamic variable, which changes over time due to the frequency drift of the local oscillator [14]. So, it is important to continuously update the clock bias.

B. Implementation

GPS time synchronization has been widely used in several applications including communications [6], sensor networks [15] and power systems [16]. Commonly, accurate time synchronization is achieved based on a timing pulse with a period of 1s. The rise time of the 1 pulse per second signal (1PPS) is synchronized with the UTC time with accuracy of a fraction of microsecond.

The 1PPS GPS signal is connected to one of the inputs of the digital controller. The rising edge of the pulse is captured by the timer module and assigned as t_{cap}. The time offset between the 1PPS signal and the local clock is computed as

$$t_{offset} = \mathrm{mod}\{t_{cap}, 1\} \tag{5}$$

in which "mod" refers to modulus. In other words, the offset time is the fractional part of the captured time. It is worth mentioning that the decimal part of t_{cap} bears no information due to periodic nature of the 1PPS signal.

The SRRF phase angle is computed as following:

$$\theta = \mathrm{mod}\left\{\omega_0\left(t - t_{offset}\right), 2\pi\right\} \tag{6}$$

in which, $\omega_0 = 2\pi f_0$ is the fundamental angular frequency. Assuming a constant and integer fundamental frequency, the angle of the SRRF at the rising edge of the 1PPS signal ($t = t_{cap}$) is zero. On the other hand, the 1PPS signal is synchronized to the global UTC time. Therefore, the SRRFs of the DERs are synchronized.

The accuracy of synchronization is dependent on the GPS receiver, the timer quantization, and the frequency drift of the local controller oscillator. The maximum phase angle error at time t can be expressed as following:

$$\theta_{err} = \omega_0\left\{e_{GPS} + e_{timer} + \int_{tGPS}^{t} F_d(\tau)\, d\tau\right\} \tag{7}$$

where, e_{GPS}, e_{timer}, F_d and t_{GPS} are the GPS receiver error, timer quantization error, frequency drift of the oscillator and the instant of time at which the last GPS pulse is captured, respectively.

The GPS and timer quantization errors are typically less than 1 microsecond. The oscillator frequency drift ranges from a few parts per billion for oven controlled crystal oscillators (OCXO) to 100 parts per million (ppm) for typical crystal oscillators. Therefore, the angle error is less than 1° with typical oscillators. However, in case that the GPS signal is interrupted, the third term on the RHS of (7) grows over time. The increase of angle error leads to circulating currents between the DERs and ultimately instability. In order to tackle this problem, a new robust control method is proposed in Section IV.

IV. Proposed Control Method

The schematic diagram of the proposed control method is shown in Fig. 2. The controller is composed of a synchronization block, which controls the reference angle of the SRRF (θ) so that the DER is synchronized with the rest of MG, a V-I droop controller, which adjusts the d and q components of the inverter reference voltage to provide even current sharing between the DERs, and cascaded voltage/current controller, which regulates the inverter reference voltage. The controller output is converted to PWM signals, which control the inverter switches. The inverter is followed by a LCL filter, which eliminates the switching harmonics.

The V-I droop controller, which was originally introduced in [10] is simple, yet fast control method, which provides a decentralized current sharing based on a global SRRF. In this method, the inverter reference voltage is adjusted according to the output current as following [17]:

$$\begin{bmatrix} v_{cd}^* \\ v_{cq}^* \end{bmatrix} = \begin{bmatrix} E_0 \\ 0 \end{bmatrix} + \begin{bmatrix} R_c & -\omega_0 L_c \\ \omega_0 L_c & R_c \end{bmatrix} \begin{bmatrix} i_d \\ i_q \end{bmatrix} - \begin{bmatrix} r_d g(i_d) \\ r_q i_q \end{bmatrix} \tag{8}$$

in which v_c^*, i, R_c, L_c, r_d, r_q are the filter capacitor reference voltage, output current, inductor resistance and inductance, the d and q axis droop coefficients, respectively. The normalized piece-wise linear function, $g()$, is introduced to improve the current sharing accuracy at high loading conditions, when the DERs are susceptible to over-current.

The first term on the RHS of (8) is the no-load reference voltage of the inverter. The second term is introduced to compensate for the voltage drop on the output inductor. The compensation improves the voltage regulation at the terminal but also improves the current sharing accuracy. The third term is a droop characteristic [10], which acts like a gain-scheduled virtual resistance [18]-[20].

In order to achieve even current sharing, the droop coefficients are selected according to the DER ratings as [21]

$$r_{d1} S_{rated1} = r_{d2} S_{rated2} = \cdots = r_{dN} S_{ratedN} \tag{9}$$

$$r_{q1} S_{rated1} = r_{q2} S_{rated2} = \cdots = r_{qN} S_{ratedN} \tag{10}$$

in which S_{ratedi} refers to the rated apparent power of unit i. Assuming, $v_{cd} \approx 1$ and $v_{cq} \approx 0$, the active (P) and reactive (Q) powers are proportional to i_d and i_q, respectively. So even current sharing implies even power sharing.

The prerequisite for the implementation of the V-I droop scheme is synchronization of the SRRFs of individual local

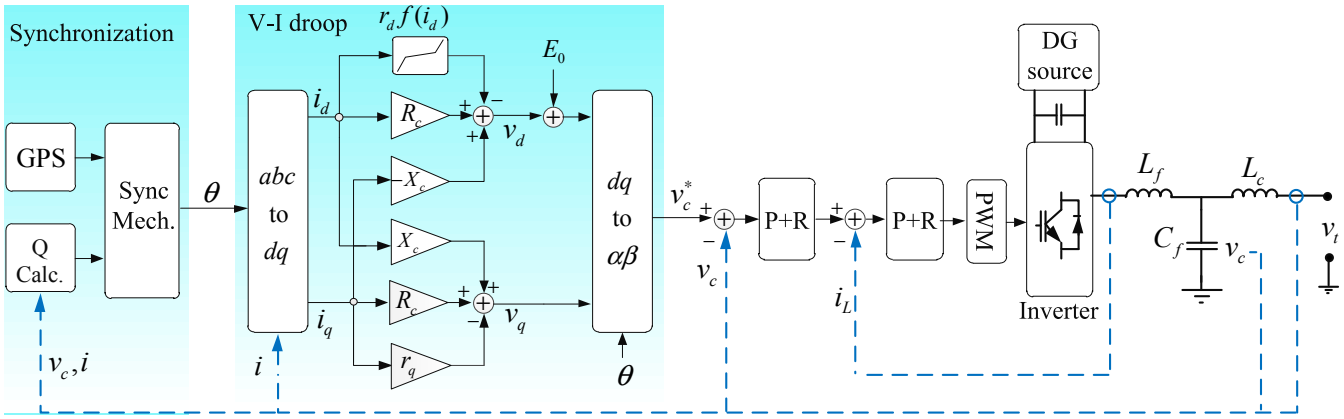

Fig. 2. Proposed control method.

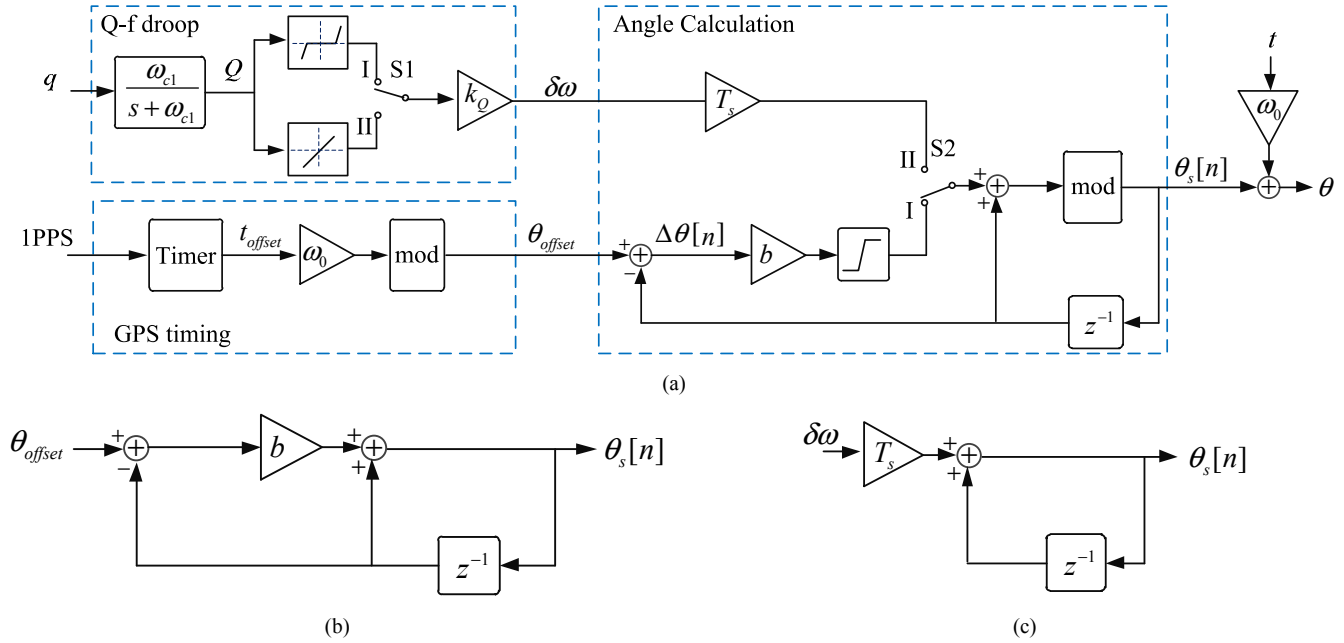

Fig. 3. Sync mechanism. (a) Block diagram. (b) Simplified angle calculation block for state 1. (c) Simplified angle calculation block for state 2.

controllers [22]. In this paper, a novel synchronization mechanism is proposed to ensure safe operation of the MG regardless of the availability of GPS signals.

The schematic diagram of the sync mechanism is shown in Fig. 3. It is composed of the GPS timing, adaptive Q-f droop and angle calculation blocks. The GPS timing block calculates the offset time between the local oscillator and the 1PPS signal from the GPS according to (5). The offset angle (θ_{offset}) is then obtained by multiplying the offset time with the fundamental frequency.

The function of the adaptive Q-f droop changes depending on the GPS signal status. When the GPS signal is present, the switch S1 is in state I. So the droop frequency ($\delta\omega$) is calculated, according to a piecewise linear characteristic as

$$\delta\omega = \begin{cases} k_Q (Q - Q_l) & \text{if } Q > Q_l \\ k_Q (Q + Q_l) & \text{if } Q < -Q_l \\ 0 & \text{otherwise} \end{cases} \tag{11}$$

where k_Q is the droop coefficient and Q_l is the reactive power limit, which is selected as a fraction of maximum permissible reactive power (e.g., Q_l=0.9Q_{max}). Equation (11) implies that while the magnitude of the reactive power is less than the limit, the droop frequency is zero and the DER operates at fixed frequency. However, if the reactive power goes beyond the range, the droop frequency is increased linearly.

In case of GPS interruption, the switch S1 is changed to state II. So the droop frequency is calculated, according to the following linear characteristic:

$$\delta\omega = \left(\frac{Q_{\max} - Q_l}{Q_{\max}} k_Q \right) Q \tag{12}$$

in which the droop coefficient is adjusted to have equal maximum droop frequency in both states.

The operation of the adaptive Q-f droop is demosntarted in Fig. 4. As for illustration, a 2 DER MG is assumed, in which DER1 (left hand side) is synchronized with the GPS receiver whereas DER2 (right hand side) is experiencing a GPS signal interruption. When the load reactive power is lower than Q_{l1} (operating point x), the frequency is fixed at f_0 and the total load reactive power is supplied by DER1. However, if the load reactive power is increased above Q_{l1}, (operating point o) the frequency rises to f_1 and the load is shared among the DERs.

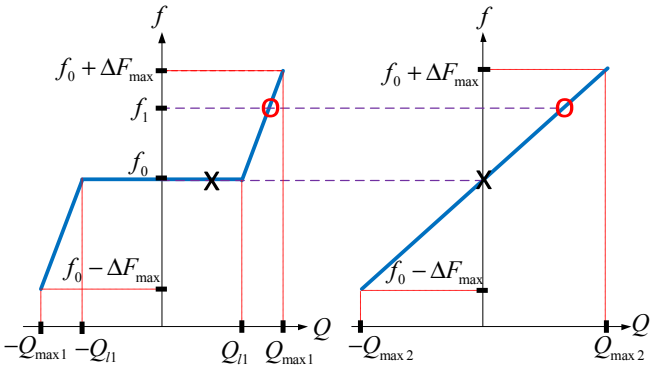

Fig. 4. Adaptive Q-f droop operation.

Therefore, each DER might operate in one of the following modes:

1- GPS is present and $|Q| \le Q_l$: frequency fixed at f_0

2- GPS is present and $|Q| > Q_l$: frequency dependent on Q

3- GPS is interrupted and $Q = 0$: frequency fixed at f_0

4- GPS is interrupted and $Q \neq 0$: frequency dependent on Q

The DERs might switch between the operating modes as a result of GPS interruption/reconnection or load changes. In order to ensure a smooth transfer between different operating modes, an angle calculation scheme is deployed.

The function of angle calculation block is controlled by switch S2. If the DER operates at mode 1, S2 is at state I. Otherwise, S2 is at state II.

In state I, the angle error ($\Delta\theta$) is obtained as the difference between the previous value of the sync angle (θ_s) and the offset angle. The angle error is then multiplied by gain b and saturated and the result is used to update the sync angle. Neglecting the saturation and mod blocks, the angle calculation block is simplified to the diagram shown in Fig. 3 (b). The sync angle can be expressed as

$$\theta_s[n] = z^{-1}\theta_s[n] + b\left(\theta_{offset}[n] - z^{-1}\theta_s[n]\right) \tag{13}$$

in which b is a constant parameter. Rearranging the terms, the block transfer function is expressed as

$$\frac{\theta_s(z)}{\theta_{offset}(z)} = \frac{b}{1-(1-b)z^{-1}} \tag{14}$$

Equation (14) represents a low pass filter with a cut-off frequency of

$$\omega_{c1} = -\frac{1}{T_s}\ln(1-b) \tag{15}$$

where T_s is the sampling period. The cut-off frequency of the low pass filter is selected considering the trade-off between smooth mode transition and time synchronization accuracy.

In case the GPS is interrupted or Q goes above Q_l, S2 is switched to state II. Neglecting the "mod" block, the angle calculation block is simplified to the diagram shown in Fig. 3 (c). So, the sync angle (θ_s) is updated, as follows:

$$\theta_s[n] = \frac{T_s}{1-z^{-1}}\delta\omega[n] \tag{16}$$

Equation (16) represents a discrete-time integrator. Therefore, the sync angle is equal to the filtered offset angle or the integral of droop frequency depending on the operating mode. The SRRF angle is calculated as the sum of the sync angle and $\omega_0 t$.

V. Small Signal Analysis of the Proposed Method

In order to study the small signal stability of the proposed method, a mathematical model of the DER is derived in this section. The inverter reference voltage is represented in the global SRRF as

$$\begin{bmatrix} v^*_{cd} \\ v^*_{cq} \end{bmatrix} = \begin{bmatrix} \cos\delta & \sin\delta \\ -\sin\delta & \cos\delta \end{bmatrix} \begin{bmatrix} v^*_{cloc,d} \\ v^*_{cloc,q} \end{bmatrix} \tag{17}$$

where v^*_{cloc} is the reference voltage in the local reference frame, which is obtained according to (8) and $\delta = \theta - \omega_0 t$ is the angle of difference between the local and global SRRFs.

Combining (17) and (8), the inverter reference voltage can be expressed as a non-linear function of the system states. Linearizing around an arbitrary equilibrium point, the function is simplified as following:

$$\Delta v^*_{cd} = V_{cq0}\Delta\delta + \left(X_c\delta_0 - r'_d\right)\Delta i_d + \left(-X_c - \delta_0 r'_q\right)\Delta i_q \tag{18}$$

$$\Delta v^*_{cq} = -V_{cd0}\Delta\delta + \left(X_c + \delta_0 r'_d\right)\Delta i_d + \left(X_c\delta_0 - r'_q\right)\Delta i_q \tag{19}$$

in which V_{cd0}, V_{cq0}, δ_0 and X_c refer to the equilibrium value of d and q axis reference voltage in the local frame, the equilibrium angle difference and the reactance of the output inductor, respectively. In addition, $r'_d = r_d f'(I_{d0}) - R_c$, $r'_q = r_q - R_c$ and I_{d0} is the equilibrium value of i_d.

The angle δ is related to the average time offset (T) and reactive power (Q) as following

$$s\delta = c_1 sT + c_2 Q \tag{20}$$

in which c_1 and c_2 are constant coefficients, which depend on the controller operating mode. Moreover, s is the derivative operator.

The average time offset and reactive power are obtained from the instantaneous values as following:

$$sT = -\omega_{c1}T + \omega_{c1}t_{offset} \tag{21}$$

$$sQ = -\omega_{c2}Q + \omega_{c2}q \tag{22}$$

$$q = v_{cd}i_q - v_{cq}i_d \tag{23}$$

in which q is the instantaneous reactive power and ω_{c2} is the cut-off frequency of the low-pass filter.

Substituting (23) into (22) and linearizing around the equilibrium point, the average reactive power is expressed as

$$s\Delta Q = -\omega_{c2}\Delta Q + \omega_{c2}\left(V_{cd0}\Delta i_q + I_{q0}\Delta v_{cd} - V_{cq0}\Delta i_d - I_{d0}\Delta v_{cq}\right) \tag{24}$$

where I_{q0} is the equilibrium value of the i_q.

The reference voltage is fed to the cascaded P+R voltage-current controllers in αβ frame. The P+R controllers can be modelled as PI controller in the SRRF frame as following [23]:

$$i^*_{Ldq} = \frac{k_{r-v}}{2s}\left(v^*_{cdq} - v_{cdq}\right) + k_{r-v}\left(v^*_{cdq} - v_{cdq}\right) \tag{25}$$

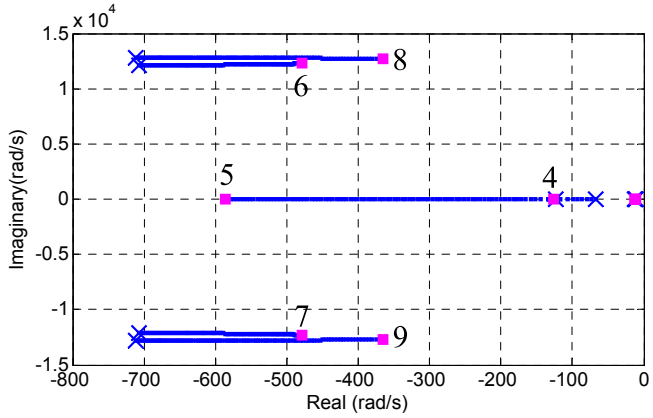

Fig. 5. Trajectory of the dominant eigenvalues for r_d varying from 2.5Ω (cross sign) to 40 Ω (square sign).

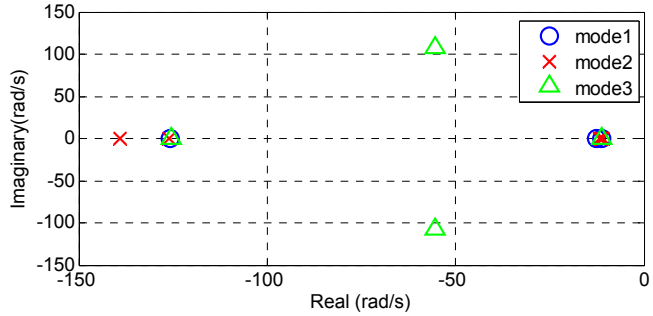

Fig. 6. Dominant eigenvalues for different modes.

$$v_{Pdq}^{*} = \frac{k_{r-i}}{2s}\left(i_{Ldq}^{*} - i_{Ldq}\right) + k_{p-i}\left(i_{Ldq}^{*} - i_{Ldq}\right) \tag{26}$$

in which $k_{r\text{-}v}$, $k_{p\text{-}v}$, $k_{r\text{-}i}$ and $k_{p\text{-}i}$ are the resonant and proportional coefficients of the voltage and current controllers, i_L^* and i_L are the reference and measured value of the filter inductor current, v_c is the filter capacitor voltage and v_p^* is the PWM reference voltage, respectively. Moreover, the subscript dq refers to the 2 element vector of d and q components.

The LCL filter dynamics are represented as

$$sL_f i_{Ldq} = -[Z_L] i_{Ldq} + v_{Pdq} - v_{cdq} \tag{27}$$

$$sC_f v_{cdq} = -[Y_c] v_{cdq} + i_{Ldq} - i_{dq} \tag{28}$$

$$sL_c i_{dq} = -[Z_c] i_{dq} + v_{cdq} - v_{tdq} \tag{29}$$

in which, $[Z_L] = \begin{bmatrix} R_L & -X_L \\ X_L & R_L \end{bmatrix}$, $[Z_c] = \begin{bmatrix} R_c & -X_c \\ X_c & R_c \end{bmatrix}$, $[Y_c] = \begin{bmatrix} 0 & -j\omega C_f \\ j\omega C_f & 0 \end{bmatrix}$, R_L is the resistance of the filter inductor, X_L is the reactance of the filter inductor, and C_f is filter capacitance.

Combining (18)-(21) and (24)-(29), the DER dynamics are expressed in state-space form as following:

$$sx = Ax + B\begin{bmatrix} v_{td} \\ v_{tq} \\ t_{offset} \end{bmatrix} \tag{30}$$

where,

$$x = \begin{bmatrix} \Delta\delta & \Delta Q & \Delta T & \Delta C_v & \Delta C_s & \Delta i_{Ldq} & \Delta v_{cdq} & \Delta i_{dq} \end{bmatrix} \tag{31}$$

in which C_v and C_s are the states of the voltage and current controllers, respectively. The system stability is studied by analyzing the eigenvalues of the matrix A. The parameters used in this study are detailed in the Section V.

The loci of the dominant eigenvalues with $c_1 = \omega_0$, $c_2 = 0$ (mode 1) and r_d varying from 1 to 50Ω are shown in Fig. 5. With the increase of r_d , the low frequency eigenvalues (4,5) move away from the imaginary axis. This result implies faster current sharing dynamics. On the other hand, the resonant eigenvalues (6-9) move towards the imaginary axis. Consequently, the LCL filter resonance becomes less damped. Therefore, there is a trade-off between the accuracy of current sharing during transients and the damping of LCL filter resonance.

The dominant eigenvalues for different operating modes are depicted in Fig. 6. It is observed that small signal stability is ensured in all operating modes.

VI. Experimental Results

The proposed control method has been implemented on a three-phase laboratory scale MG, as shown in Fig. 7. The test MG is composed of three inverter-based DERs, three loads and a resistive line model. A variable DC voltage source is used to supply the inverters. Electronically controlled circuit breakers are used to connect/disconnect the inverters and loads from the MG.

The test MG is composed of two experimental setups, which are connected in parallel. The DER1 is included in setup 1 and DERs 2 and 3 are included in setup 2. Each setup is equipped with a dSPACE 1006 controller platform. The dSPACE controllers are connected to PCs using Ethernet interface. The "dSPACE Control Desk" program is used to manage the dSPACE controllers and plots/save the signals. The experimental results are captured using the "dSPACE control desk" and plotted in MATLAB.

In order to demonstrate the performance of GPS time synchronization, two Securecync ® GPS receivers from Spectracom are utilized. The GPS receivers, which are specifically designed for time synchronization purposes, generate a TTL compatible 1PPS square wave signal. The 1PPS signals from the GPS receivers are depicted in Fig. 8. It is observed that the 1PPS signals are synchronized with an accuracy of less than 1μs. The 1PPS signal is captured by dSPACE I/O interface card (DS4002) and used by local controllers to calculate the offset time between the individual local controller clock and the global UTC time (t_{offset}).

The specifications of the experimental hardware as well as control parameters are listed in Table II. The MG is operated at frequency of 50Hz and phase voltage of 220Vrms. The inverters have a rating of 2kVA and are switched at PWM frequency of 10kHz. The load impedances are selected so that the full load power is close to the MG capacity. The LV feeder is modelled by resistive line impedances.

The droop coefficients r_d and k_Q are selected based on the permissible voltage and frequency deviations, respectively. The q axis droop coefficient is then designed based on the

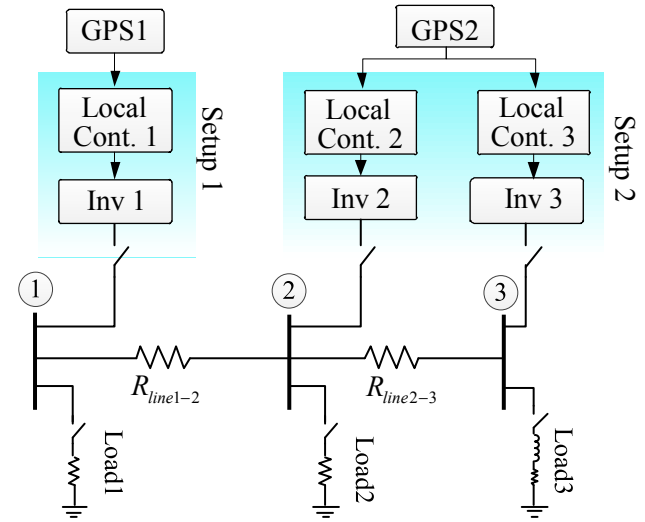

(a)

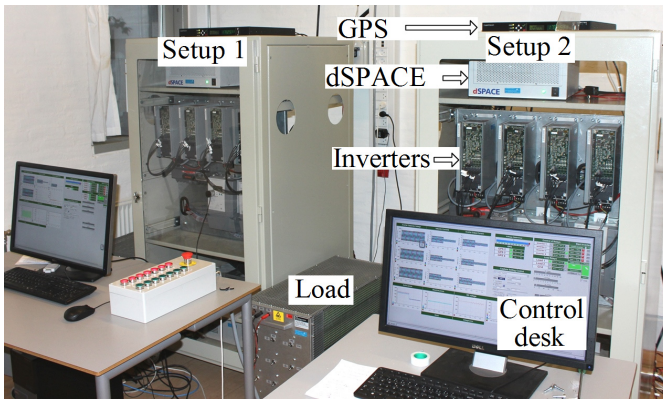

(b)

(c)

Fig. 7. Experimental setup. (a) Schematic diagram, (b) Hardware and (c) GPS receiver.

small signal analysis of Section IV. The voltage and current controller parameters are designed based on structured H∞ method [24].

In order to study the performance of the proposed method, four tests are conducted:

1. Step load change with the P-V/Q-f droop method
2. Step load change with the proposed method
3. Connection of a DER to the MG
4. GPS signal interruption and reconnection

With the aim of presenting a comparative study, the P-V/Q-f droop method [25], which is conventionally used for MGs with resistive lines, is implemented. The conventional droop parameters are listed in Table III. The P-V and Q-f droop coefficients are designed based on the permissible voltage deviations and pole placement method, respectively. The step load response with the conventional droop method is depicted in Fig. 9. Initially, loads 1 and 2 are connected. At t=0.05s, a large reactive load is connected to bus 3. Following the load rise, the active and reactive powers experience overshoot and ringing. The poor dynamic response is mainly originated from the power measurement delay. Moreover, the active power sharing is less accurate at higher loading conditions due to the larger voltage drops on the lines. As a result, the DER3, which is closer to the load, experiences a current overshoot as illustrated in Fig. 9 (c).

TABLE II
PARAMETERS OF THE TEST MG

Description	Parameter	Value	Unit
Fundamental Frequency	f_0	50	Hz
Rated phase Voltage	V_{rated}	220	Vrms
Inverter Specifications	S_{rated}	2	kVAR
	f_{PWM}	10	kHz
LCL Filter	L_f	8.6	mH
	C_f	4.5	μF
	L_c	1.8	mH
Load impedances	R_1	115	Ω
	R_2	153	Ω
	Z_3	43+j22	Ω
Line Impedances	$R_{line1-2}$	0.66	Ω
	$R_{line2-3}$	0.22	Ω
V-I droop coefficients	r_d	6.5	Ω
	r_q	25	Ω
Q-f droop parameters	kQ	0.3	Hz/kVAR
	ω_{c2}	50 π	rad/s
	$Qmax$	1	kVAR
	Ql	0.9	kVAR
Voltage controller parameters	k_{p1}	0.008	S
	kr_1	36	S/s
Current controller parameters	k_{p2}	45	Ω
	k_{r2}	1000	Ω/s
Sync mechanism LPF	ω_{c1}	4π	rad/s
	b	0.00125	-

TABLE III
PARAMETERS OF THE CONVENTIONAL DROOP

Parameter	Value	Unit
P-V droop coefficient	0.014	1/A
Q-f droop coefficient	0.012	Hz/kVAR

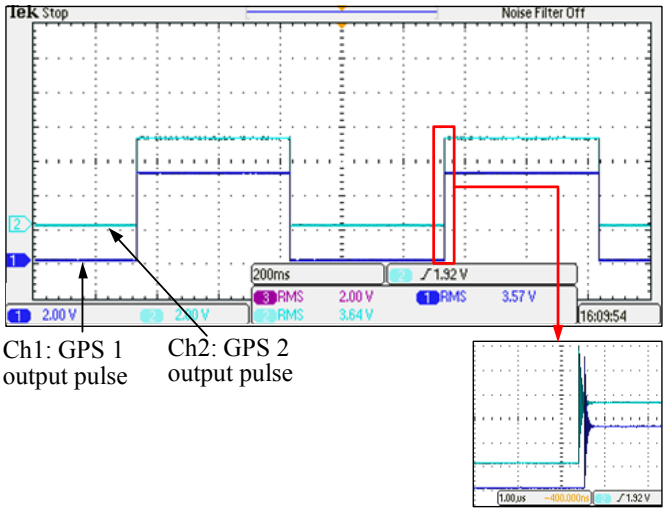

Fig. 8. 1PPS signals from measured from GPS receivers outputs.

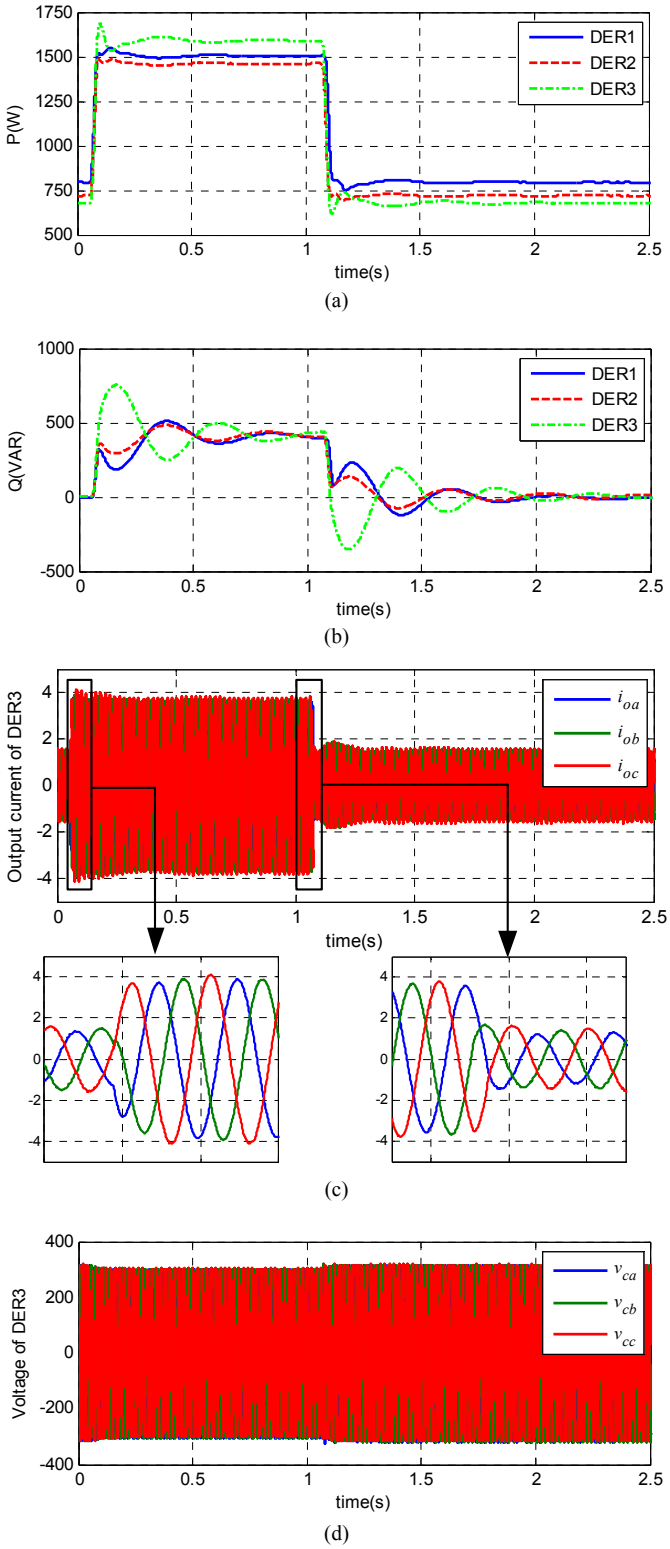

Fig. 9. Experimental Results for test 1 (conventional method). (a) Active powers. (b) Reactive powers. (c) Current of DER3. (d) Voltage of DER3.

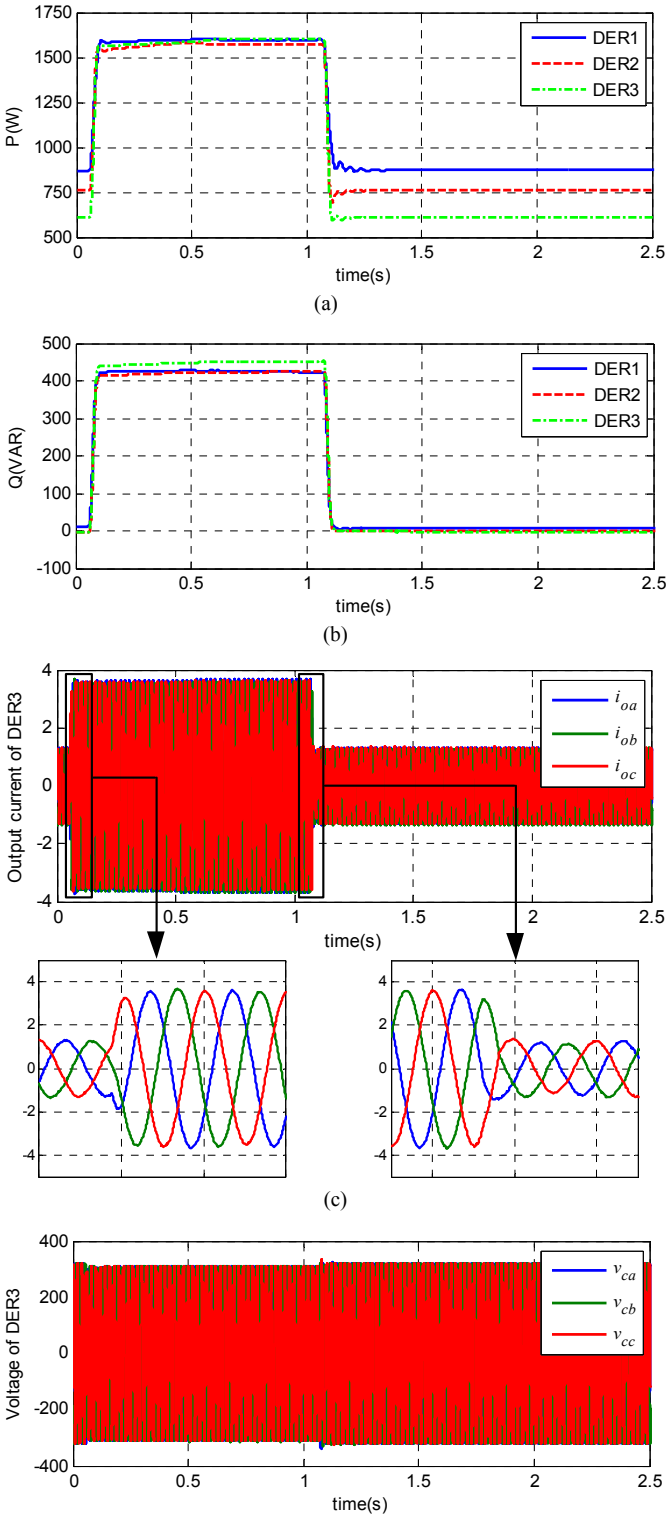

Fig. 10. Experimental Results for test 2 (proposed method). (a) Active powers. (b) Reactive powers. (c) Current of DER3. (d) Voltage of DER3.

The step load response with the proposed method is depicted in Fig. 10. Comparison of Fig. 9 and 10 reveals a significant improvement of the dynamic response. Specifically, the transient response of active and reactive power is smooth and the settling time is less than a cycle. As a result, the current of DER 3 rises smoothly. In addition, the active power sharing is more accurate at high loading conditions thanks to the piece-wise linear V-I droop characteristics. This helps preventing DERs from overload. Furthermore, the rms voltage is within the permissible range (0.95pu to 1.05 pu), as depicted in Fig. 10 (d).

The experimental results for DER connection test are shown in Fig. 11. Initially, DER1 and load 1 are connected to the MG. At t=0.05s, DER 2 is connected. It is observed that the load power is shared between the DERs following the connection. The transient of active power and current is smooth and the reactive power remains constant. Therefore, the proposed method enables smooth connection of DERs to

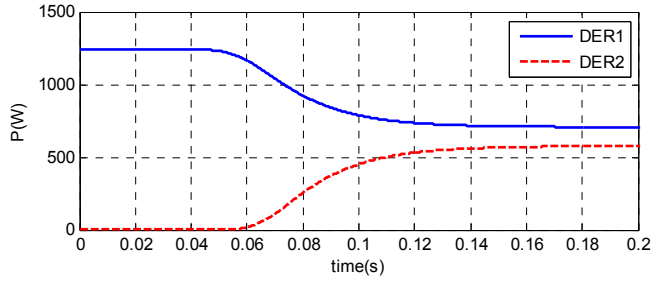

(a)

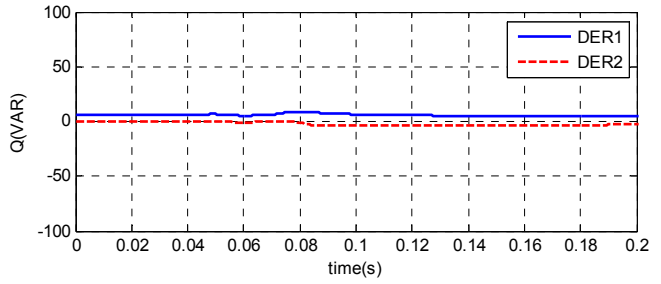

(b)

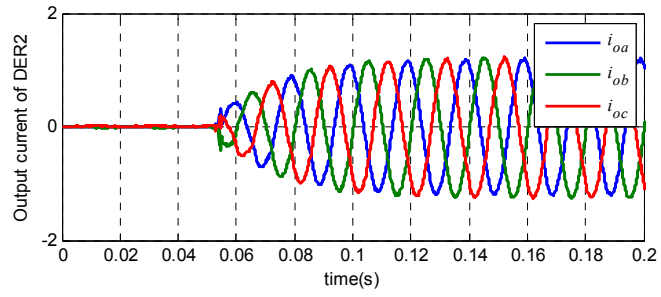

(c)

Fig. 11. Experimental Results for test 3. (a) Active powers. (b) Reactive powers. (c) Current of DER2.

the MG without requirement for additional synchronization mechanisms (such as PLL).

The experimental results for test 4 are illustrated in Fig. 12. Initially, all of the DERs and loads are connected to the MG and all GPS receivers are active. At t=5s, the GPS signal of DER1 is manually interrupted. So, DER1 uses the linear Q-f droop characteristics to maintain synchronization with DERs 2 and 3. Since DERs 2 and 3 keep the system synchronized to the UTC time, the frequency is fixed at 50Hz. So, Q_1 drops to zero and Q_{load} is shared between DERs 2 and 3 according to the v_q-i_q droop characteristics.

At t=25s, the GPS signal of DER2 is interrupted. Following, DER3 attempts to keep the frequency fixed. However, since the Q_{load} is higher than the Q_l, the DER3 is switched to mode 2, changing the frequency according to the piece-wise linear Q-f characteristics. Consequently, Q_1 and Q_2 rise and Q_3 is retained below the maximum value. At t=45s, the GPS of DER 3 is interrupted. As a result, DER3 is also changed to linear droop characteristics. So, Q_{load} is equally shared between the DERs.

At t=65s and 75s, load 3 is disconnected and connected, respectively. It is observed that the step load response is smooth despite the GPS interruptions. At t=90s, the GPS signal of DER 2 is reconnected, changing the DER2 to mode2. At t=110s, the GPS signal of DER1 is reconnected. At this stage, Q_2 drops below Q_l and the DERs 1 and 2 synchronize the MG with the UTC time. As a result, the frequency is changed back to 50Hz and Q_3 drops to zero. At t=140s, the

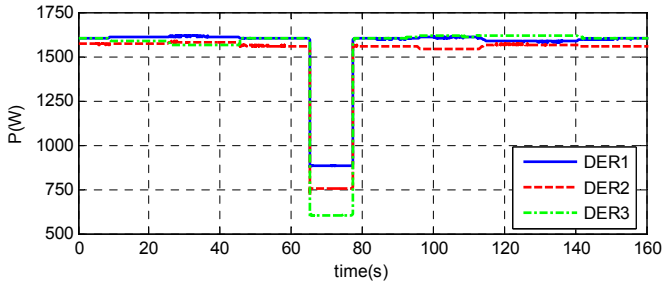

(a)

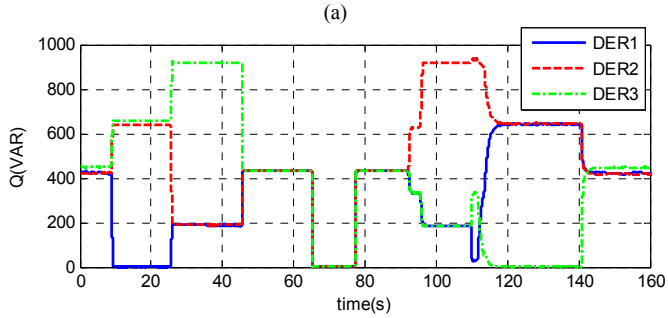

(b)

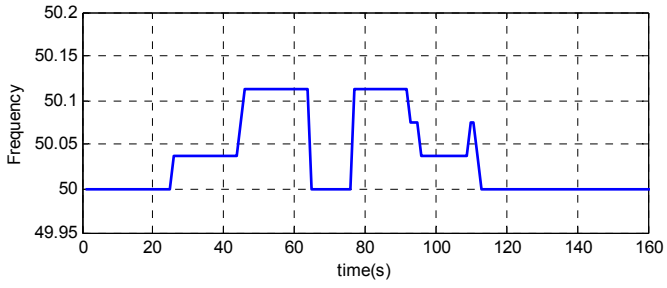

(c)

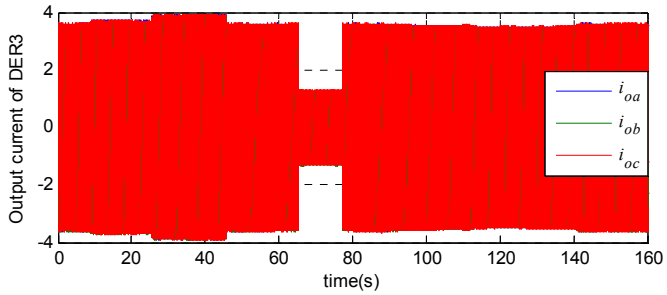

(d)

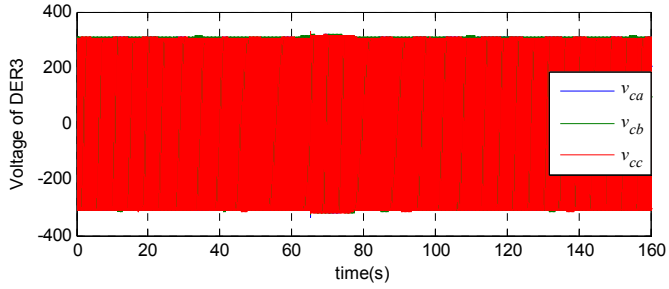

(e)

Fig. 12. Experimental Results for test 4. (a) Active powers. (b) Reactive powers. (c) Frequency. (d) Current of DER3. (e) Voltage of DER3.

GPS of DER3 is also connected, switching the DER to mode 1. Subsequently, the reactive power is equally shared between the DERs.

Experimental results show that in case of GPS disconnection/reconnection, the DERs change their operating modes so as to maintain synchronization with the MG but also enable fast step load response regardless of the GPS availability. In terms of power quality, fixed frequency

operation is achieved as long as sufficient number of DERs receiving the GPS signals. In addition, the voltage profile of the MG is within the permissible range of 0.95 to 1.05pu.

VII. Conclusions

In this paper, a novel decentralized control method is proposed to for inverter-based islanded MGs. In this method, the SRRFs of the DERs are synchronized to a common reference frame by means of a sync mechanism, which uses a combination of GPS timing and an adaptive Q-f droop controller to align the reference angle of the DERs. In order to coordinate the active and reactive power generation of DERs and follow the load changes with a fast dynamic response, the DER voltage is adjusted according to the V-I droop characteristics.

The proposed control method has been tested using a laboratory-scale MG. The experimental results demonstrate that the proposed method favors from the following features:

- Fixed frequency operation as long as a sufficient number of GPS receivers are functional
- Robustness with respect to GPS signal interruptions
- Overdamped step load response, which eliminates current overshoots
- Improved active power and current sharing at high loading conditions
- Simple connection of the DERs to the MG
- Voltage profile within the permissible range

The proposed method in this paper opens up a new way to integrate the GPS technology with the state of the art control methods in MGs. A future step is using GPS for measuring the phase angle of harmonic currents and developing advanced control methods for harmonic current sharing.

References

[1] J. M. Guerrero, M. Chandorkar, T. Lee, and P. C. Loh, "Advanced Control Architectures for Intelligent Microgrids ; Part I: Decentralized and Hierarchical Control," *IEEE Trans. Ind. Electron.,* vol. 60, pp. 1254-1262, Apr. 2013.

[2] A. Bidram and A. Davoudi, "Hierarchical Structure of Microgrids Control System," *IEEE Trans. Smart Grid,* vol. 3, pp. 1963-1976, May 2012.

[3] J. Rocabert, A. Luna, F. Blaabjerg, Rodri, x, and P. guez, "Control of Power Converters in AC Microgrids," *IEEE Trans. Power Electron* ,. vol. 27, pp. 4734-4749, Nov. 2012.

[4] Q. Shafiee, J. M. Guerrero, and J. C. Vasquez, "Distributed Secondary Control for Islanded Microgrids-A Novel Approach," *IEEE Trans. Power Electron.,* vol. 29, pp. 1018-1031, Feb. 2014.

[5] C. Ahumada, R. Cardenas, D. Saez, and J. M. Guerrero, "Secondary Control Strategies for Frequency Restoration in Islanded Microgrids With Consideration of Communication Delays," *IEEE Trans. Smart Grid,* Early access, DOI 10.1109/TSG.2015.2461190.

[6] W. Lewandowski, J. Azoubib, and W. J. Klepczynski, "GPS: primary tool for time transfer," in *Proc. of the IEEE,* vol. 87, pp. 163-172, 1999.

[7] R. Majumder, A. Ghosh, G. Ledwich, and F. Zare, "Angle droop versus frequency droop in a voltage source converter based autonomous microgrid," in *Proc. Power & Energy Society General Meeting, (PES),* 2009, pp. 1-8.

[8] A. H. Etemadi, E. J. Davison, and R. Iravani, "A Decentralized Robust Control Strategy for Multi-DER Microgrids - Part I: Fundamental Concepts," *IEEE Trans. Power Del.,* vol. 27, pp. 1843-1853 ,Sept. 2012.

[9] S. Riverso, F. Sarzo, and G. Ferrari-Trecate, "Plug-and-Play Voltage and Frequency Control of Islanded Microgrids With Meshed Topology," *IEEE Trans. Smart Grid,* vol. 6, pp. 1176-1184, May 2015.

[10] M. S. Golsorkhi and D. D. C. Lu, "A Control Method for Inverter-Based Islanded Microgrids Based on V-I Droop Characteristics," *IEEE Trans. Power Del.,* vol. 30, pp. 1196-1204, Jun. 2015.

[11] H. Jinwei, L. Yun Wei, J. M. Guerrero, F. Blaabjerg, and J. C. Vasquez, "An Islanding Microgrid Power Sharing Approach Using Enhanced Virtual Impedance Control Scheme," *IEEE Trans. Power Electron.,* vol. 28, pp. 5272-5282, Nov. 2013.

[12] R. Majumder, "Some Aspects of Stability in Microgrids," *IEEE Trans. Power Syst.,* vol. 28, pp. 3243-3252, Aug. 2013.

[13] P .Moore and P. Crossley, "GPS applications in power systems. I. Introduction to GPS," *Power Engineering Journal,* vol. 13, pp. 33-39, Feb. 1999.

[14] Y. Quan and G. Liu, "Compensation Local Clock_s Drift by Timestamp Stream," in *Proc. Innovative Computing, Information and Control*, 2007, pp. 524-524.

[15] S. M. Lasassmeh and J. M. Conrad, "Time synchronization in wireless sensor networks: A survey," in Proc. *IEEE SoutheastCon (SoutheastCon)*, 2010, pp. 242-245.

[16] M. Jaya Bharata Reddy, D. V. Rajesh, P. Gopakumar, and D. K. Mohanta, "Smart Fault Location for Smart Grid Operation Using RTUs and Computational Intelligence Techniques," *IEEE Systems Journal,* vol. 8, pp. 1260-1271, Dec. 2014.

[17] M. S. Golsorkhi and D. D. C. Lu, "A decentralized power flow control method for islanded microgrids using V-I droop," in *Proc. Iranian Conference on Electrical Engineering (ICEE)*, 2014, pp. 604-609.

[18] Y. Zhu, Z. Fang, F. Wang, B. Liu, R. Gou, and Y. Zhao, "A Virtual Impedance Optimization Method for Reactive Power Sharing in Networked Microgrid," *IEEE Trans. Power Electron.,* vol. 31, pp. 2890 - 2904, Jun. 2015.

[19] H. Mahmood, D. Michaelson, and J. Jin, "Accurate Reactive Power Sharing in an Islanded Microgrid Using Adaptive Virtual Impedances," *IEEE Trans. Power Electron.,* vol. 30, pp. 1605-1617, Mar. 2015.

[20] L. Yun Wei and K. Ching-Nan, "An Accurate Power Control Strategy for Power-Electronics-Interfaced Distributed Generation Units Operating in a Low-Voltage Multibus Microgrid," *IEEE Trans. Power Electron.,* vol. 24, pp. 2977-2988, Dec. 2009.

[21] M. S. Golsorkhi Esfahani and D. D. C. Lu, "A Decentralized Control Method for Islanded Microgrids under Unbalanced Conditions," *IEEE Trans. Power Del.,* vol. Early access, DOI: 10.1109/TPWRD.2015.2453251, 2015.

[22] M. S. Golsorkhi and D. D. C. Lu, "A decentralized negative sequence compensation method for islanded mirogrids," in *Proc. International Symposium on Power Electronics for Distributed Generation Systems (PEDG)*, 2015, pp. 1-7.

[23] R. Teodorescu, F. Blaabjerg, M. Liserre, and P. C. Loh, "Proportional-resonant controllers and filters for grid-connected voltage-source converters," *Electric Power Applications, IEE Proceedings,* vol. 153, pp. 750-762, 2006.

[24] A. M. Bouzid, M. S. Golsorkhi, P. Sicard, and A. Cheriti, "H structured design of a cascaded voltage/current controller for electronically interfaced distributed energy resources," in *Proc. International Conference on Ecological Vehicles and Renewable Energies (EVER),* 2015, pp. 1-6.

[25] J. M .Guerrero, J. Matas, V. Luis Garcia de, M. Castilla, and J. Miret, "Decentralized Control for Parallel Operation of Distributed Generation Inverters Using Resistive Output Impedance," *IEEE Trans. Ind. Electron.,* vol. 54, pp. 994-1004, Apr. 2007.

Mohammad S. Golsorkhi (S'13) received the B.Sc. (Hons.) degree in electrical engineering from Isfahan University of Technology, Isfahan, Iran, in 2009 and the M.Sc. (Hons.) degree in electrical engineering from Tehran Poly-echnique, Tehran, Iran, in 2012. During 2011-2012, he worked in Behrad consulting engineers as a R&D engineer. His responsibilities included project management, design of power electronics devices, and power quality analysis for major industries. He is currently pursuing the PhD degree in electrical engineering at The University of Sydney, Australia. In 2015, he was a visiting PhD student with the Department of Energy Technology, Aalborg University, Denmark. His current research interests include control of microgrids, renewable energy resources, and power electronics.

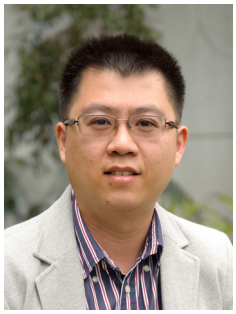

Dylan Dah-Chuan Lu (S'00 – M'04 – SM'09) received his B.Eng. (Hons.) and Ph.D. degrees in Electronic and Information Engineering from The Hong Kong Polytechnic University, Hong Kong in 1999 and 2004 respectively.

In 2003, he joined PowereLab Ltd. as a Senior Design Engineer. His major responsibilities included project development and management, circuit design, and contribution of research in power electronics. Since 2006, he has been with the School of Electrical and Information Engineering, The University of Sydney, Australia, where he is currently an Associate Professor. He was a Visiting Associate Professor at the University of Hong Kong in 2013. He is the author and co-author of over 130 papers in the areas of power electronics and engineering education. He has two patents on efficient power conversion. His current research interests include power electronics circuits and control for efficient power conversion, lighting, renewable electrical energy systems, microgrids, motor drive and power quality improvement, and engineering education.

Dr. Lu is a member of the Institute of Engineers Australia. He presently serves as an Associate Editor for the IEEE Transactions on Circuits and Systems II. He also serves as an Associate Editor for the IET Renewable Power Generation and the International Journal of Electronics. He served as a Guest Editor for the IEEE Transactions on Industrial Electronics; special issue on Power Converters, Control and Energy Management for Distributed Generation in July 2015 issue.

Josep M. Guerrero (S'01-M'04-SM'08-FM'15) received the B.S. degree in telecommunications engineering, the M.S. degree in electronics engineering, and the Ph.D. degree in power electronics from the Technical University of Catalonia, Barcelona, in 1997, 2000 and 2003, respectively. Since 2011, he has been a Full Professor with the Department of Energy Technology, Aalborg University, Denmark, where he is responsible for the Microgrid Research Program. From 2012 he is a guest Professor at the Chinese Academy of Science and the Nanjing University of Aeronautics and Astronautics; from 2014 he is chair Professor in Shandong University; from 2015 he is a distinguished guest Professor in Hunan University; and from 2016 he is a visiting professor fellow at Aston University, UK.

His research interests is oriented to different microgrid aspects, including power electronics, distributed energy-storage systems, hierarchical and cooperative control, energy management systems, smart metering and the internet of things for AC/DC microgrid clusters and islanded minigrids; recently specially focused on maritime microgrids for electrical ships, vessels, ferries and seaports. Prof. Guerrero is an Associate Editor for the IEEE TRANSACTIONS ON POWER ELECTRONICS, the IEEE TRANSACTIONS ON INDUSTRIAL ELECTRONICS, and the IEEE Industrial Electronics Magazine, and an Editor for the IEEE TRANSACTIONS on SMART GRID and IEEE TRANSACTIONS on ENERGY CONVERSION. He has been Guest Editor of the IEEE TRANSACTIONS ON POWER ELECTRONICS Special Issues: Power Electronics for Wind Energy Conversion and Power Electronics for Microgrids; the IEEE TRANSACTIONS ON INDUSTRIAL ELECTRONICS Special Sections: Uninterruptible Power Supplies systems, Renewable Energy Systems, Distributed Generation and Microgrids, and Industrial Applications and Implementation Issues of the Kalman Filter; the IEEE TRANSACTIONS on SMART GRID Special Issues: Smart DC Distribution Systems and Power Quality in Smart Grids; the IEEE TRANSACTIONS on ENERGY CONVERSION Special Issue on Energy Conversion in Next-generation Electric Ships. He was the chair of the Renewable Energy Systems Technical Committee of the IEEE Industrial Electronics Society. He received the best paper award of the IEEE Transactions on Energy Conversion for the period 2014-2015. In 2014 and 2015 he was awarded by Thomson Reuters as Highly Cited Researcher, and in 2015 he was elevated as IEEE Fellow for his contributions on "distributed power systems and microgrids."